

TOPICAL PAPER

Microbial Surfaces Investigated Using Atomic Force Microscopy

Anastassia V. Bolshakova,[†] Olga I. Kiselyova,^{*,‡} and Igor V. Yaminsky^{†,‡}

Faculties of Chemistry and Physics, M.V. Lomonosov Moscow State University, GSP-2, Leninskie gory, 119992, Moscow, Russia

This paper is dedicated to atomic force microscopy (AFM) as a progressive tool for imaging bacterial surfaces and probing their properties. The description of the technique is complemented by the explanation of the method's artifacts typical, in particular, for the imaging of bacterial cells. Sample preparation techniques are summarized in a separate section. Special attention is paid to the differences in imaging of Gram-positive and Gram-negative bacteria. Probing of mechanical properties, including elastic modulus, fragility, and adhesion of the cell walls is emphasized. The advantages of AFM in the studies of real-time cellular dynamical processes are illustrated by the experiment with the germination of spores.

Introduction

Invented in 1986 (1), atomic force microscope (AFM) soon conquered a leading position in all fields of surface science, including biological investigations. This occurred as a result of several specific features of the technique. Here we will discuss those related to biological and particularly microbiological applications. Providing the topography of surfaces at nanometer scale, AFM at the same time makes it possible to study cells in air or liquid environment, avoiding any staining or placement of them in ultrahigh vacuum. Time-lapse observations in liquid environment permit monitoring of dynamic processes such as cell growth and division, spore resuscitation, etc. AFM technique combines microscopy in its conventional understanding with the ability to study the object's mechanical (2, 3), immunochemical (4), adhesive (5), and electrostatic (6) properties at the nanoscale level. Recent technical achievements will allow for the use of fluorescent biomarkers, registered on a single-molecule level by means of AFM and a near-field optical microscope hybrid device. All of these aspects make AFM an outstanding technique for microbiological research. On the other hand, bacteria are also favorable objects for AFM as a result of their properties. Typical dimensions of bacterial whole cells (1–5 μm) are suitable for commercially available microscopes, whereas surface features are easily detectable with the necessary resolution (7). Bacteria are surrounded by a cellular wall, and therefore their surface is much more rigid than that of animal cells; this fact simplifies AFM study.

Atomic Force Microscopy

The atomic force microscope is one of the scanning probe microscope (SPM) family members. The easiest

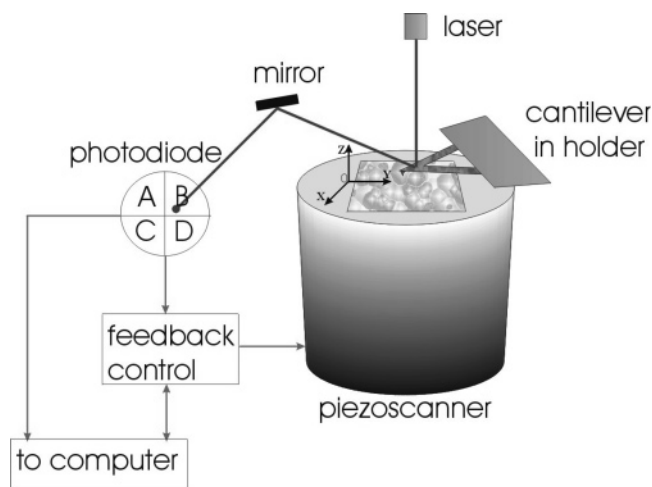


Figure 1. Schematic illustration of the AFM technique.

way to describe it is to say that AFM is a micro profilometer of the surface, with high resolution, which can reach atomic level (e.g., on atomic-flat surfaces). A simple scheme of the AFM mechanical parts is shown in Figure 1. The AFM probes the surface by scanning with a tip, mounted at the end of a thin, flexible, cantilever placed in a holder, across the sample, while the electronic system registers and the computer records cantilever position Z in each point of the surface with coordinates (X, Y) . Alternatively, the tip can stay immobile, whereas the sample will be scanned in the X, Y directions, as shown in the scheme (Figure 1). Such scheme is used in many commercially available models of the AFM. For biological applications in modern Bio-AFM, a scheme with a mobile tip is used. When the tip (probe) is brought close to the surface, forces occurring between them cause the deflection of the cantilever, which is registered and transferred into an electric signal. The optical detection system consists of a laser beam directed to the reflective surface of the cantilever and a four-sectional photodiode,

* To whom correspondence should be addressed. E-mail: ok@polly.phys.msu.ru.

[†] Faculty of Chemistry.

[‡] Faculty of Physics.

which measures both vertical and lateral displacements. Vertical deflection Δz is proportional to the overall force acting normally between the tip and the sample, according to Hooke's law $F_{\text{sum}} = k\Delta z$, k being the cantilever spring constant. The torsional deformation of the cantilever, resulting into the lateral displacement of the laser beam, is proportional to the friction force between the tip and the sample existing during scanning.

AFM operates in several regimes. In the topographic (or "constant force") mode, the cantilever deflection (and therefore the probe-sample force) is maintained constant by means of the feedback loop. The interaction force strongly depends on the tip-sample distance and is determined by adhesion, van der Waals, and capillary interactions. Provided the interatomic interaction is uniform, the cantilever Z position reflects the topography of the sample, i.e., its height. The typical AFM image representation is similar to a geographical map, where the color corresponds to the relief height. The computer software transforms the information from the piezoscanner into a three-dimensional image.

In the so-called "deflection mode" (or "error signal mode") the vertical deflection of the cantilever is mapped. This regime outlines minor details of the sample, and the data are often acquired simultaneously with topographical ones. This mode is especially favorable for objects possessing both high and low topographical features, such as bacteria (see below).

Topographical data can be obtained not only through permanent contact between the tip and the sample, i.e., in the contact mode (1) described above, but also in the dynamic resonant mode (8). In the resonant mode, the cantilever is forced to oscillate with its resonance frequency. In the vicinity of the surface, the resonant frequency is shifted as a result of tip-surface interaction, resulting in amplitude reduction with respect to the free oscillations. In this regime, the tip taps the surface in the lowest point of oscillation. During scanning the feedback system modulates the cantilever holder vertical position so that to maintain constant amplitude. The cantilever position follows the topography of the studied surface. Depending on the technical realization, particularly, on how the oscillations are urged, the resonant regime can be called "tapping mode" or MAC (magnetic alternating current) mode (9). In tapping mode, the oscillations are driven by the piezoelement incorporated in the tip holder. In MAC mode the tip is covered by a magnetic material and oscillates in the external alternating magnetic field.

The force modulation regime can be used to detect variations in a surface's mechanical properties. In the force modulation mode the cantilever is forced to oscillate while the tip remains in contact with the sample surface. This can be achieved by either oscillating the cantilever with the resonant frequency of the cantilever holder, or oscillating the sample in the vertical direction. During the scanning, the value of indentation changes in accordance with the local elasticity of the sample. Imaging a stiffer area of the sample results in a smaller surface depth of the indentation and, therefore, oscillation amplitude of the tip compared to those over a compliant one (10).

Force Imaging. To measure the force between the probe and the sample a so-called "force curve" is recorded. In force curve regime the probe is moved in the Z direction, normal to the surface. First it moves toward the surface until it comes into contact, and then goes backward, till no interaction between the surface and the probe is sensed.

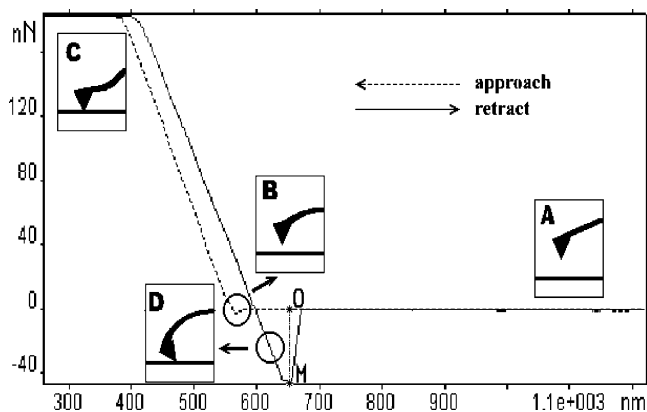


Figure 2. Force curve, recorded on a bacterium's surface

Force curves contain lots of information on surface properties such as local Young's modulus, adhesion between the tip and the surface (for a review, see ref 11). A typical example of a force curve is given in Figure 2: (A) When the tip is far from surface the interaction force between them can be neglected, i.e., it equals zero. (B) When the tip approaches the surface (dotted line), and the attractive force becomes sufficient, the cantilever deflects toward the surface. (C) When the tip comes into contact with the surface, the cantilever deflects due to repulsion force. The more we push the holder toward the surface, the more it deflects. When the tip and the rigor surface are in contact, the force curve can be roughly described by the linear plot, in accordance with Hooke's law, $F = k\Delta Z$, where ΔZ and k are the deflection and the spring constant of the cantilever, respectively. This part of the force curve can be used for the determination of local elasticity properties, in particular, local Young's modulus of the surface material. When the cantilever holder moves away from the surface (solid line), the tip is not separated from the surface at once (D). Adhesive forces between the surface and the tip keep them in contact, which causes deflection of the cantilever, since the holder is moving away. When the elastic force pulling the tip away from the surface reaches the value of the adhesive force, the tip detaches from the surface and the cantilever returns to the initial position (A).

The value of the adhesion force between the tip and the sample is determined as the value of segment OM in Figure 2.

However, it should be noted that force curve measurement has several limitations. First of all, AFM does not conduct direct measurements of the distance between the sample and the tip; therefore, the determination of "zero" axes is a very complicated problem. Besides, for "soft materials" it is difficult to separate the relative contributions to the cantilever deflection from surface forces and deformation of the sample.

Sample Preparation

Though practically each new object is a unique task for AFM investigation and one can choose a new immobilization method, here we describe several preparation strategies for imaging of bacteria in both liquid and air environments. The most common and easiest substrates in use for bacteria immobilization are mica, glass, or polystyrene and Millipore filters (12). Indium tin oxide glasses were used in one of the first experiments on imaging of *E. coli* in tapping mode (13).

A droplet of bacterial suspension (5–10 μL) is placed onto the chosen substrate and left to expose for several minutes. The concentration of bacteria suspension is

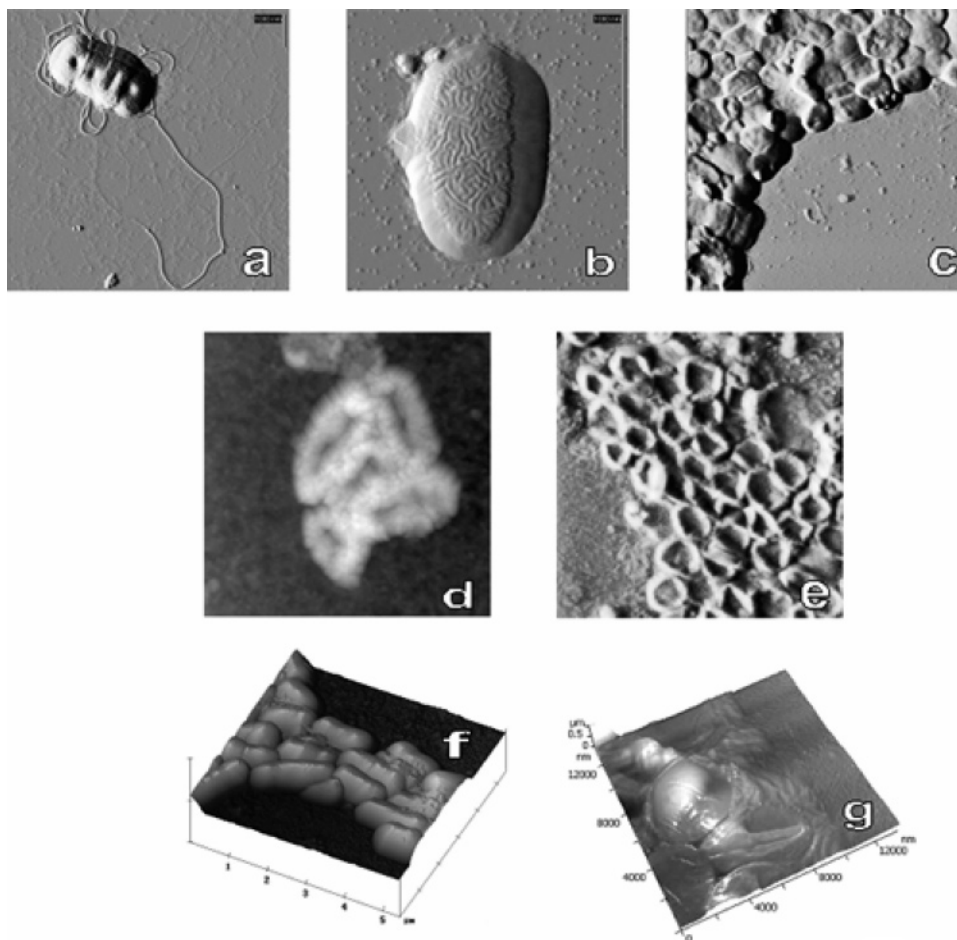


Figure 3. AFM images of bacteria of different taxonomy groups: (a) highlighted image of bacteria *E. coli* SO4, image size $8 \times 8 \mu\text{m}^2$; (b) highlighted image of bacterium *Klebsiella pneumoniae* 711, image size $2 \times 2 \mu\text{m}^2$; (c) highlighted image of bacteria *Azotobacter* sp., image size $13 \times 13 \mu\text{m}^2$. (d) height image of bacteria *Rhodococcus luteus*, image size $4 \times 4 \mu\text{m}^2$; (e) highlighted image of bacteria *Micrococcus luteus*, image size $6 \times 6 \mu\text{m}^2$; (f) 3D image of bacteria *Helicobacter pylori*, image size $5.5 \times 5.5 \mu\text{m}^2$; (g) 3D image of bacteria *Pseudomonas* sp., image size $13 \times 13 \mu\text{m}^2$. All images (a–g) were obtained in air.

about 10^8 – 10^9 /mL. The exact concentration depends on the adhesive properties of bacteria and has to be adjusted for each case.

For AFM experiments in air, samples are left to dry in ambient air. Interestingly, many of such samples, if stored properly, can be imaged months and even years afterward. Images of bacteria of different taxonomy groups are presented in Figure 3. It was shown that drying of certain bacteria does not affect them. Several in situ imaging techniques, invoking rehydrataion of immobilized bacteria after short drying, take advantage of that fact (14).

AFM experiments in liquid media require more stable immobilization of bacteria on the substrate surface and, therefore, surface preparation. The most common approaches are polycationic treatment and coating with agarose (15) or MRS (Man, Rogosa, and Sharpe) broth (14). Trapping of cells in the pores of Millipore membranes (16, 17) is another technique that allows the study of bacterial surfaces. Though this technique does not permit measurement of the cells' height and, therefore, part of the morphological information can be lost, nevertheless it has proved to be perfect for force measurements, revealing mechanical and adhesive properties of the cells.

The most popular polycationic treatment is the formation of a polylysine adlayer. For polylysine treatment (18) a $10\text{-}\mu\text{L}$ drop of 10^{-2} M polylysine solution is applied onto freshly cleaved mica plates and left to dry. Polylysine

adsorbs to mica and gives a smooth coverage in the form of a monolayer, composed of tightly packed globules with RMS roughness 1.0–1.5 nm. Such coverage is inappropriate for imaging individual macromolecules but is smooth enough for imaging “huge” objects, such as bacteria. Polylysine is biocompatible and should not affect bacteria. The technique described above was applied for the studies of the surface morphology of two strains *E. coli* (JM 109 and K12 J62) (18). A similar technique of bacteria fixation on a polylysine-covered glass surface was successfully used for imaging of *E. coli* DH5a and *Listeria ivanovii* CIP 7842T in both air and culture medium (19). Another easily preparable polycationic coating for glass, polyethyleneimine, can be used for *E. coli* contact AFM experiments in liquid (20).

To obtain agarose coating (15), 200–500 mg of agarose solution in 2–5 mL of water was heated for full dissolving, and then a drop of solution was put onto freshly cleaved mica and left for 5–10 min. A droplet of bacterial suspension was then set onto the substrate surface. Agarose coverage on mica provides a surface consisting of small globules, which is smooth enough to allow bacteria cell visualization. The cells are partially depleted into the substrate, which provides stable fixation for experiments in liquid media.

A set of more complicated techniques including covalent bonding of bacterial cells to the substrates through protein–protein cross-linking reaction is described in ref 21.

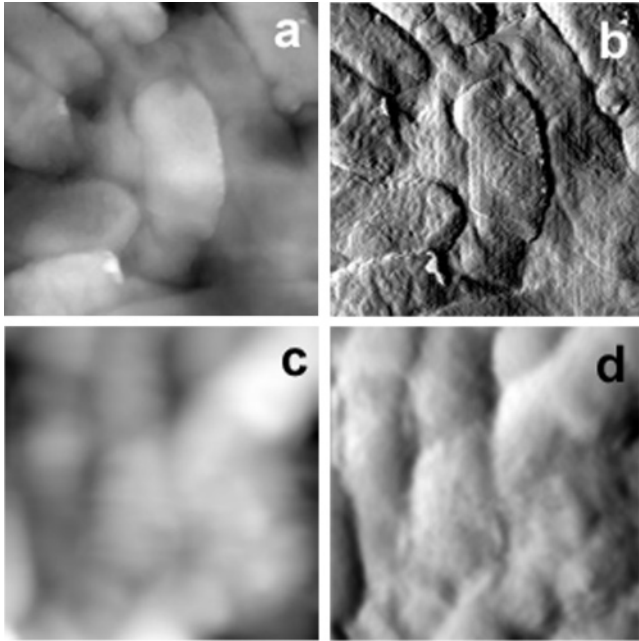


Figure 4. AFM images of *Escherichia coli* JM109: (a, b) in air; (c, d) in liquid; (a, c) height image; (b, d) highlighted image. Image size $3 \times 3 \mu\text{m}^2$.

AFM Imaging of Bacteria

Difference in Imaging of Gram-Positive and Gram-Negative Bacteria. The Gram-accessory of the bacterium is one of the key points in AFM imaging of bacteria. Imaging of Gram-positive bacteria in both air and liquid environments reveals their surface topographic features. Surface layers (S-layers) of certain bacteria consist of protein subunits forming highly ordered lattices with different symmetries. A classical example of such structure is the hexagonally packed intermediate layer of *Deinococcus radiodurans* (22). The curvature of bacterial shape often distorts high-resolution AFM images of structures with crystalline packing. To avoid this effect, 2D crystal HPI layer sheets were removed from the surface of *D. radiodurans* and imaged on a flat mica substrate (23). A similar approach yielded AFM images of regular S-layer protein sheets with 4-fold lattice symmetry removed from the surface of the Gram-positive bacterium *Bacillus sphaericus* by lysozyme treatment (24). The high-resolution (2 nm) images of *Lactobacillus helveticus* S-layer were obtained in situ before and after denaturing by LiCl (14).

The imaging environment is critical for the appearance of Gram-negative bacteria in AFM. Typically, bacterial cells imaged in liquid are devoid of surface topographic features (Figure 4) (18), registered on the same cells after drying. Normally, properly prepared samples of Gram-positive bacteria in liquid environment provide resolution not worse than that of dried ones (22). Thus, the reason for such "resolution failure" most likely lies in the dynamics of cellular filaments, carbohydrate chains of lipopolysaccharides, that form on the outer surface of Gram-negative bacteria (25, 26).

Interestingly, for Gram-negative bacteria, the dimensions of cells depend on the environment. In liquid, their heights (200–500 nm) and widths (1100–1500 nm), depending on the strain, exceed considerably (150–250 nm) their respective dimensions in air (18, 27). (See refs 18 and 27 for tables providing detailed comparison of dimensions in different environments for various strains.) It's important to note that for Gram-positive bacteria this

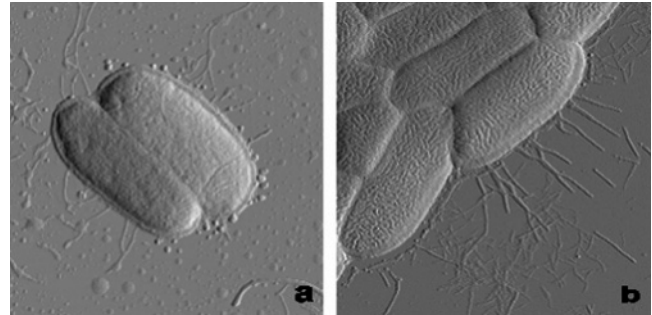


Figure 5. AFM images of *E. coli* parent (a) and gene-modified (b) transductant strain K12 J62, acquiring *Shigella flexneri* O-antigen (group-specific factor 3,4 rfb-a3,4) strains of *E. coli*. Image size is $3 \times 3 \mu\text{m}^2$. Images were obtained in air. The images are reproduced from ref 28.

effect was not reported. Presumably, the height and width reduction in air is due to drying of polysaccharide gel on the surface of bacteria. After drying, these inherent features of bacterial cells are collapsed onto the wall surface, creating a strain-specific topography of the surface.

Genetically Linked Strains. Genetic modification of bacterial strains for practical applications has become a routine procedure for molecular biologists. The most common biotechnological example is the expression of proteins. Directed modifications of genes responsible for the synthesis of surface lipopolysaccharide chains (O-antigenes) can be undertaken in order to produce living vector vaccines, i.e., noninfectious strains carrying certain O-antigenes of infectious ones. Such cells are mistaken by the immune system for infectious ones and can be used for immunization.

Changes of surface polysaccharide structure can be registered by means of AFM (28). AFM images of the cell surface of *E. coli* parent strain K12 J62 and *E. coli* transductant strain K12 J62, acquiring the capacity for synthesizing primary S-specific side chains of the lipopolysaccharide of *Shigella flexneri* O-antigen (group-specific factor 3,4 rfb-a3,4) (Figure 5), revealed the presence of essential differences in cell surface pattern. The surface of the mutant strain carrying rfb-a3,4 of *S. flexneri* (Figure 5b) is highly structured, being formed of densely packed lamellae 30–40 nm in diameter and 200 nm long. The parental strain surface is practically devoid of lamellar structures and consists of round-shaped ones.

Surface alterations in genetically modified strains of *Staphylococcus aureus* associated with the vancomycin-resistant strains were observed using the simplest technique of drying a droplet of suspension on glass surface (29). Two parallel circumferential surface rings were revealed on the surface of glycopeptide-intermediate *S. aureus* clinical strain and its revertant. In vancomycin-susceptible strains, additional rings were formed in the presence of vancomycin.

Various types of surface damage caused by antibiotic treatment of bacteria could be directly observed in AFM preparations (30).

Immunochemical Approach. Specifically bound antibodies, forming monolayers on the surface of bacteria, can be easily detected by means of AFM. Labeling of bacterial surfaces with specific antibodies to surface lipopolysaccharides (LPS) facilitates strain identification. The outer membrane integrity was tested by immunolabeling, making it possible to distinguish the outer membrane LPS from the peptidoglycan layer (25).

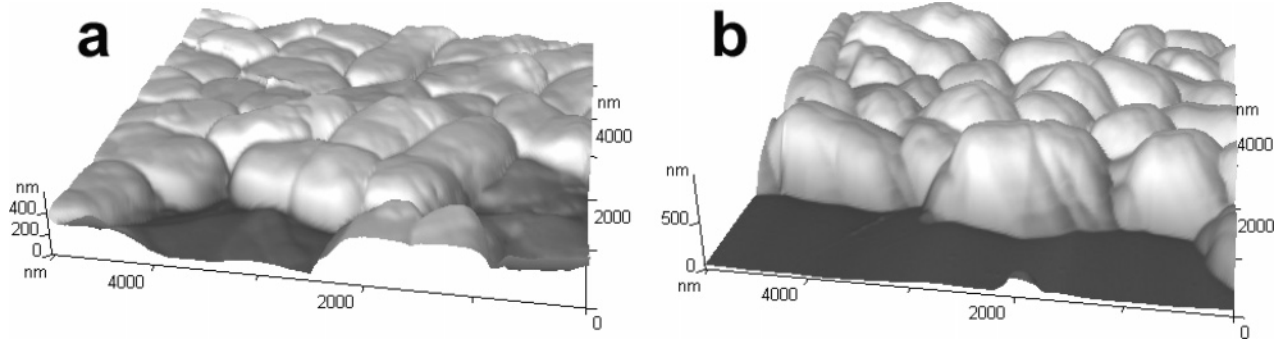


Figure 6. 3D image of bacteria *Arthrobacter globiformis* in vegetative (a) and mummy (b) state. Images were obtained in air.

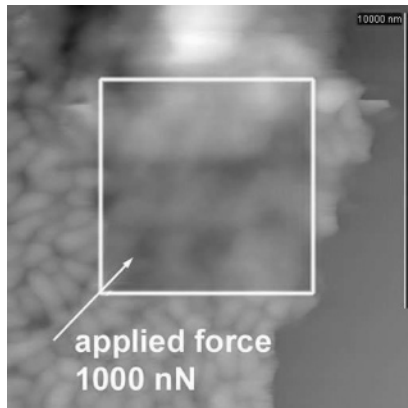


Figure 7. Illustration of destructive effect of applied force on *Arthrobacter globiformis* bacteria. The image was obtained in air. For details, see ref 15.

Fragility of Bacterial Cellular Walls. Being a force probe technique, AFM not only “sees” topographical surface properties but also probes mechanical characteristics of bacterial surface, i.e., the cellular wall. The difference in cellular wall fragility can be demonstrated considering the example of vegetative and mummy forms of *Arthrobacter globiformis* 235-2 (31).

Vegetative bacteria were grown for 4 days at 37 °C. The mummified bacteria were anabiotic cells produced from vegetative ones by the treatment with the auto-regulator, factor *d1* (artificial analog—alkyloxybenzene group, potassium salt, concentration 0.15%). For further investigation, the standard method of sample preparation was used (see above). Evidently, the height of the vegetative bacteria was less than that of the mummies (Figure 6). Force modulation experiments were carried out for comparing of the stiffness of the outer bacterial shell.

In force modulation regime, the force applied to sample surface was about 1 μ N, using the cantilever with a spring constant of 48 N/m. After prolonged scanning in force modulation regime, the applied force being almost 100 times more than in typical topographical experiments, mummy bacteria were destroyed (small square region with destroyed cells in Figure 7), whereas vegetative ones remained visually unchanged. This result demonstrates that *A. globiformis* are relatively fragile in the mummy state and are stiffer in the vegetative state.

Force–Distance Probing. Force–distance curves recorded over bacterial surfaces contain lots of information on local adhesive and mechanical properties. Processing of such data using the theory of deformation allows measurement of not only Young’s modulus of bacteria (32) but even bacterial turgor pressure (33). Adhesive and mechanical properties of *Azotobacter chroo-*

coccum and *Bacillus cereus*, fixed on the surface and probed by silicon nitride tip, were compared in ref 15. Alternatively, adhesive properties can be measured by fixing bacteria on the AFM tip and probing different surfaces (34). Such approach is favorable for measurements of the adhesive forces between cells and minerals (35).

(a) Adhesion. Force curves over the studied surfaces need to be recorded in liquid media to avoid capillarity effects. For *Azotobacter chroococcum* in vegetative form two peaks characterizing adhesion and probe takeoff were registered (indicated by arrows Figure 8a). One of them is located in the contact area, whereas the other one is approximately 120 nm higher. This distance corresponds to the length of O-antigens’ polysaccharide chains on the surface of Gram-negative bacteria. Presumably, the first peak is due to the interaction with the cell wall and the second is due to the free ends of O-antigens, whereas the probe moves in the polysaccharide gel while between them. Force curves for mummies of *A. chroococcum* have only one adhesion peak, located in the contact area. Transformation into mummy form invokes processes that destroy the polysaccharide layer. Gram-positive bacteria *B. cereus* in both vegetative cell and spore forms demonstrated one peak of adhesion (Figure 8b).

Adhesion maps were recorded for unsaturated biofilms formed by *Pseudomonas putida*, indicating that the spaces between cells were less adhesive than the surfaces of the cells (36).

(b) Young’s Modulus. The slope of force curves, s , recorded on bacteria by means of AFM is related to bacteria’s effective spring constant k_b via a simple formula $k_b = ks/(1 - s)$, where k is the cantilever’s spring constant (37). Effective spring constants of various bacterial strains have been determined by several groups, obtained typical values in buffer solutions being 0.03–0.05 N/m for *E. coli* K12 (38) and 0.04–0.07 N/m for *Magnetospirillum gryphiswaldense* (33).

Meanwhile, the effective spring constant is an integral characteristic of a cell as a whole and not of the surface material itself. To elucidate the elastic modulus (Young’s modulus) of the bacterial surface, Hertz’s model of elastic deformations can be applied (39, 40). For *Azotobacter chroococcum* the calculations after measurements in liquid yielded the value of Young’s modulus of 6×10^8 Pa in the vegetative phase and 9×10^8 Pa in the mummy phase. For *B. cereus* this value measured under the same conditions was smaller, 1.5×10^8 and 1.0×10^8 Pa in the vegetative and spore phases, respectively. Measurements of elastic modulus of *B. subtilis* in air provide values from 3×10^7 Pa at 95% humidity to 1.3×10^{10} Pa at 20% humidity (41). For hydrated yeast cells of *Saccharomyces cerevisiae* Young’s modulus for the bud scar

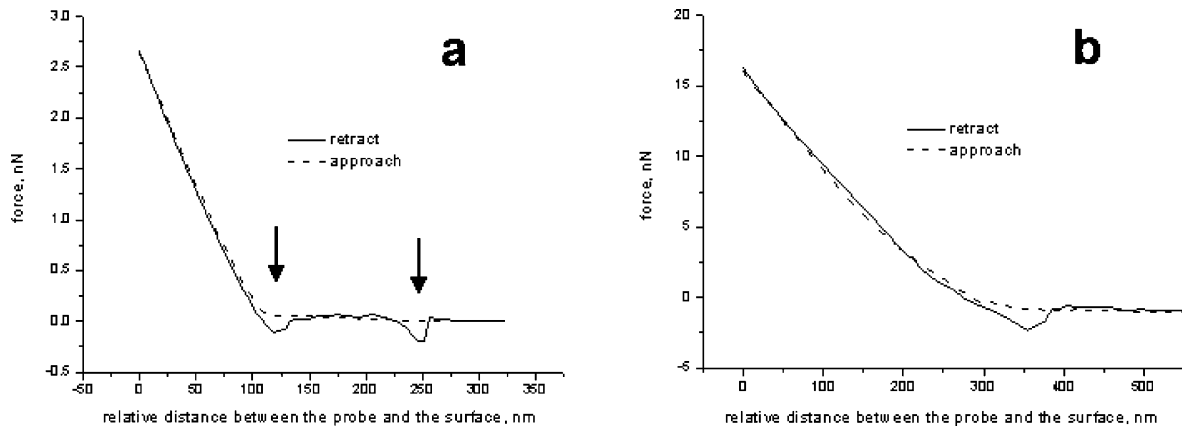


Figure 8. AFM force curves recorded on bacterial surface: (a) force curve recorded on *Azotobacter chroococcum* vegetative; arrows indicate peaks due to adhesion; (b) force curve recorded on *Bacillus cereus* spore. Cantilever rigidity constant is 0.12 N/m.

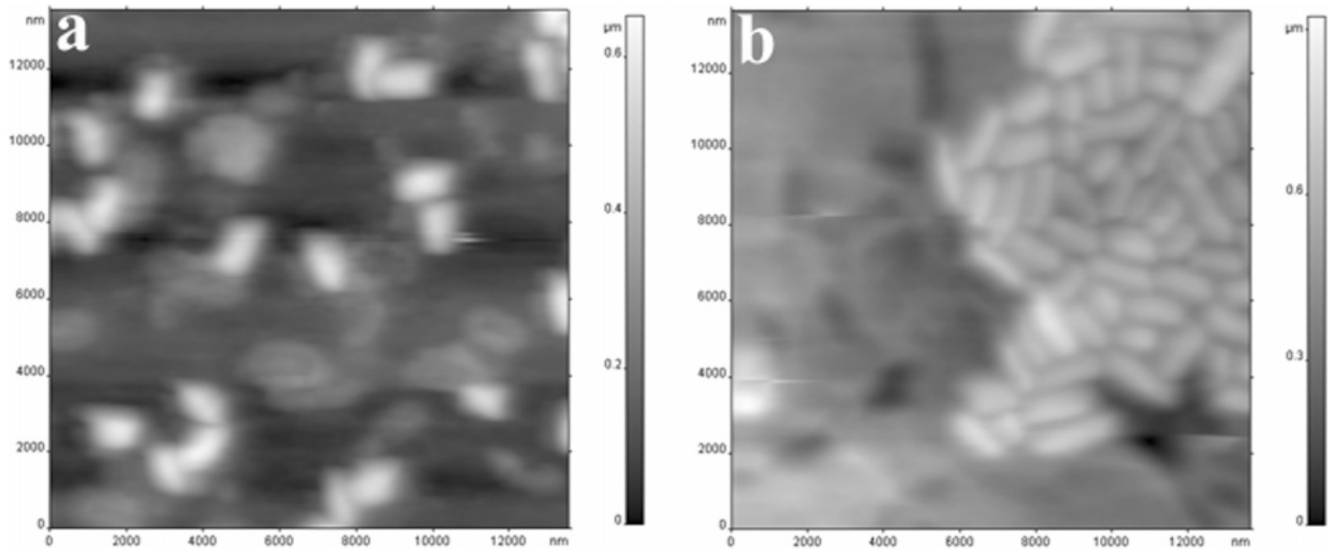


Figure 9. Growth of *Bacillus* sp. bacterial spores: (a) control image in air, $t = 0$; (b) vegetative form, $t = 4$ h 45 min. Images were obtained in buffer solution before and after addition of nutrients. For details see ref 15.

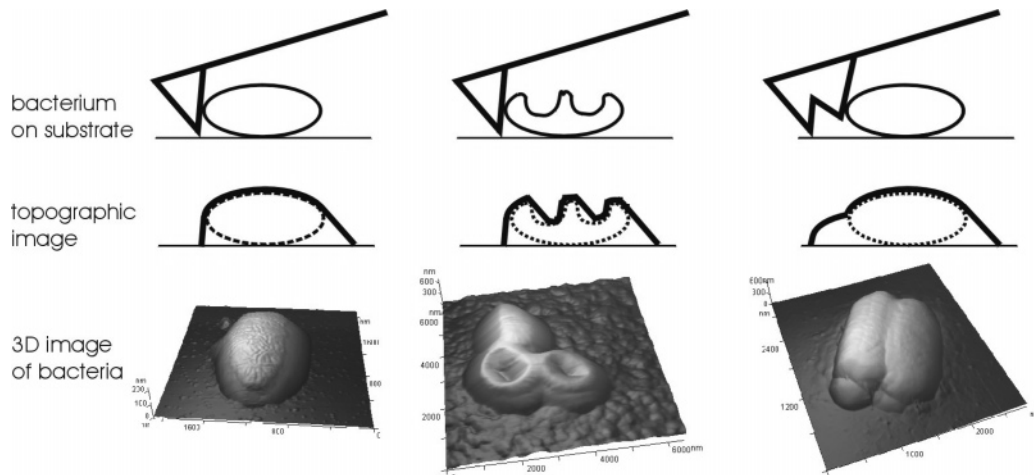


Figure 10. Illustration of the origin of “side-wall” artifacts.

and surrounding cell surface in water was estimated using the Hertz model to be 1–2 orders of magnitude less, i.e., $(6.1 \pm 2.4) \times 10^6$ and $(0.6 \pm 0.4) \times 10^6$ Pa, respectively (42). All of the obtained values for bacteria are of the same order of magnitude, 10^7 – 10^8 Pa, typical for many polymeric glasses.

An elegant method of measuring the elastic modulus of bacterial surface material is based on spreading the

extracted membrane (43) or murein sacculi (44) on a solid material with narrow grooves and pushing it into a groove by the AFM tip. The main advantage of this technique is that the parameters of the cell are not involved in the calculations. This method yielded a value of the elastic modulus in the range of 3.3 – 3.9×10^{10} Pa for *Methanospirillum* sheath in air (43), and 3 – 4×10^8 Pa for dried sacculi of Gram-negative bacteria (44).

The main drawback of all AFM deformation measurements is that calculations involve the exact shape of the AFM tip, which is usually not known exactly.

Bacterial Spore Germination. AFM analysis of *Bacillus* sp. spore surfaces carried out by means of AFM in aqueous solutions revealed a series of bumps on the coat surfaces, as well as a series of ridges, most of which were oriented along the long axis of the spore (45).

Imaging in liquid opens vast perspectives for in situ monitoring of dynamic processes such as cell growth, division, and movement. An interesting example is the germination of *Bacillus* sp. from spores into vegetative cells (15). After recording control images of *Bacillus* sp. on agarose-coated mica (Figure 9a), nutrients were injected into the AFM liquid cell. After 30 min of incubation at room temperature the dimensions of bacteria cells increased; 5–6 h later grown spores disappeared and small vegetative cells were seen instead (Figure 9b). Interestingly, “new-born” vegetative cells formed a biofilm.

Artifacts. Like many other experimental techniques, the AFM method is not devoid of artifacts. One of the most important ones is broadening and consequent distortion of the AFM image profile.

The AFM probe has finite dimensions, and accordingly the apparent lateral dimensions of the object are overestimated (46, 47). If the adsorbed object is relatively high for probe microscopy (about several microns) and the edge of the object goes up abruptly, only the top region of the bacteria will be imaged correctly. This is the facet of the probe but not its sharp end that contacts with the sidewall of the object and the AFM image comes out as a superposition of the two profiles (tip and object), so the image of the side regions of bacteria will be corrupted. Figure 10 illustrates the impact of the probe geometry on the acquired images of the cells. If there are two or more tips instead of a single one on the probe extremity, the image of the sample contains a “double-image” artifact. A “high” object has a shadow or multishadow (Figure 10). A simple geometrical model of tip–bacteria contact is described in ref 48.

Summary

Atomic force microscopy is a quickly developing analytical method for biological, medical, and cosmetology applications (49). In vitro studies of bacterial cells are performed in different environmental conditions, including buffer solutions. Both 3D imaging and probing of local mechanical properties of cells may be used for the purposes of descriptive bacteriology. The study of the bacterial response to the different reagents may be used in clinical practice for earlier diagnostics of bacterial infections and development of effective ways to defeat the disease. The possible combination of atomic force microscopy with high-resolution fluorescent optical microscopy will benefit the efficiency of medical treatment.

Acknowledgment

We thank the reviewers for their valuable suggestions. All AFM images were analyzed by FemtoScan Online Image Processing Software (50). Financial support from INTAS (grant N 01-0045) and NATO Science Program (grant N LST.CLG.980194) is greatly acknowledged.

References and Notes

- Binnig, G.; Quate, C. F.; Gerber, C. Atomic Force Microscopy. *Phys. Rev. Lett.* **1986**, *56*, 930–933.
- Domke, J.; Radmacher, M. Measuring the Elastic Properties of Thin Polymer Films with the Atomic Force Microscope. *Langmuir* **1998**, *14*, 3320–3325.
- A-Hassan, E.; Heinz, W. F.; Antonik, M. D.; D’Costa, N. P.; Nageswaran, S.; Schoenenberger, C.-A.; Hoh, J. H. Relative Microelastic Mapping of Living Cells by Atomic Force Microscopy. *Biophys. J.* **1998**, *74*, 1564–1578.
- Hinterdorfer, P.; Baumgartner, W.; Gruber H. J.; Schilcher, K.; Schindler, H. Detection and Localization of Individual Antibody–Antigen Recognition Events by Atomic Force Microscopy. *Proc. Natl. Acad. Sci. U.S.A.* **1996**, *93*, 3477–3481.
- Chen, X.; Davies, M. C.; Roberts, C. J.; Tendler, S. J. B.; Williams, P. M. Recognition of Protein Adsorption onto Polymer Surfaces by Scanning Force Microscopy and Probe-Surface Adhesion Measurements with Protein-Coated Probes. *Langmuir* **1997**, *13*, 4106–4111.
- Rotsch, C.; Radmacher, M. Mapping Local Electrostatic Forces with the Atomic Force Microscope. *Langmuir* **1997**, *13*, 2825–2832.
- Tollersrud, T.; Berge, T.; Andersen, S. R.; Lund, A. Imaging the Surface of *Staphylococcus aureus* by Atomic Force Microscopy. *Acta Pathol. Microbiol. Immunol. Scand.* **2001**, *109*, 541–545.
- Zhong, Q.; Inniss, D.; Kjoller, K.; Elings, V. B. Fractured Polymer/silica Fiber Surface Studied by Tapping Mode Atomic Force Microscopy. *Surf. Sci. Lett.* **1993**, *290*, L688–L692.
- Han, W.; Lindsay, S. M.; Jing, T. A Magnetically Driven Oscillating Probe Microscope for Operation in Fluids. *Appl. Phys. Lett.* **1996**, *69*, 4111–4114.
- Maivald, P.; Butt, H.-J.; Gould, S. A. C.; Prater, C. B.; Drake, B.; Gurley, G.; Elings, V. B.; Hansma, P. K. Using Force Modulation to Image Surface Elasticities with the Atomic Force Microscope. *Nanotechnology* **1991**, *2*, 103–106.
- Zlatanova, J.; Lindsay, S. M.; Leuba, S. H. Single Molecule Force Spectroscopy in Biology Using the Atomic Force Microscope. *Prog. Biophys. Mol. Biol.* **2000**, *74*, 37–61.
- Kasas, S.; Fellay, B.; Cargnello, R. Observation of Action of Penicillin on *Bacillus subtilis* using Atomic Force Microscopy: Technique for the Preparation of Bacteria. *Surf. Interface Anal.* **1994**, *21*, 400–401.
- Shibata-Seki, T.; Watanabe, W.; Masai, J. J. Imaging of the Cells with Atomic Force Microscopy Operated at a “Tapping” Mode. *J. Vac. Sci. Technol., B* **1994**, *12*, 1530–1534.
- Sokolov, I. Y.; Firtel, M.; Henderson, G. S. In situ High-resolution Atomic Force Microscope Imaging of Biological Surfaces. *J. Vac. Sci. Technol., A* **1996**, *14*, 674–678.
- Bolshakova, A. V.; Vorobyova, E. A.; Yaminsky, I. V. Indication of Living Bacterial Cells in Native Soil and Permafrost. *Phys. Low-Dim. Struct.* **2003**, *3/4*, 105–112.
- Dufrene, Y. F.; Boonaert, Ch. J. P.; Gerin, P. A.; Asther, M.; Rouxhet, P. G. Direct Probing of the Surface Ultrastructure and Molecular Interactions of Dormant and Germinating Spores of *Phanerochaete chrysosporium*. *J. Bacteriol.* **1999**, *181*, 5350–5354.
- van der Mei, H. C.; Busscher, H. J.; Bos, R.; de Vries, J.; Boonaret, C. J. P.; Dufrene, Y. F. Direct Probing by Atomic Force Microscopy of the Cell Surface Softness of a Fibrillated Oral Streptococcal Strain. *Biophys. J.* **2000**, *78*, 2668–2674.
- Bolshakova, A. V.; Kiselyova, O. I.; Filonov, A. S.; Frolova, O. Yu.; Lyubchenko, Yu. L.; Yaminsky, I. V. Comparative Studies of Bacteria with Atomic Force Microscopy Operating in Different Modes. *Ultramicroscopy* **2001**, *68*, 121–128.
- Robichorn, D.; Girard, J.-C.; Centiempo, Y.; Cavellier J.-F. Atomic Force Microscopy Imaging of Dried or Living Bacteria. *C. R. Acad. Sci., Ser. III* **1999**, *322*, 687–693.
- Razatos, A.; Ong, Y.-L.; Sharma, M. M.; Georgiou, G. Molecular Determinants of Bacterial Adhesion Monitored by Atomic Force Microscopy. *Appl. Biol. Sci.* **1998**, *95*, 11059–11064.
- Camesano, T. A.; Natan, M. J.; Logan, B. E. Observation of Changes in Bacterial Cell Morphology Using Tapping Mode Atomic Force Microscopy. *Langmuir* **2000**, *16*, 4563–4572.
- Lister, T. E.; Pinhero, P. J. In Vivo Atomic Force Microscopy of Surface Proteins on *Deinococcus radiodurans*. *Langmuir* **2001**, *17*, 2624–2628.

- (23) Muller, D. J.; Baumeister, W.; Engel, A. Conformational Change of the Hexagonally Packed Intermediate Layer of *Deinococcus radiodurans* Monitored by Atomic Force Microscopy. *J. Bacteriol.* **1996**, *178*, 3025–3030.
- (24) Wahl, R.; Raff, J.; Selenska-Pobell, S.; Mertig, M.; Pompe, W. A Fast Screening Method for Surface Layers on Gram-Positive Bacteria. *Biotechnol. Lett.* **2001**, *23*, 1485–1490.
- (25) Amro, N. A.; Kotra, L. P.; Wadu-Mesthrige, K.; Bulychev, A.; Mobashery, S.; Liu, G. High-resolution Atomic Force Microscopy Studies of the *Escherichia coli* Outer Membrane: Structural Basis for Permeability. *Langmuir* **2000**, *16*, 2789–2796.
- (26) *Bergey's Manual of Determinative Bacteriology*, 9th ed.; Holt, J. G., Ed.; Williams & Wilkins: Baltimore, 1994.
- (27) Lomonosov, A. M.; Egorov, S. N.; Gallyamov, M. O.; Yaminsky, I. V. AFM of Bacterial Cells Subjected to Different Factors. *Phys. Low-Dim. Struct.* **2003**, *3/4*, 125–130.
- (28) Yaminsky, I. V.; Demin, V. V.; Bondarenko, V. M. The Differences in Cellular Surface of Hybrid Bacteria *Escherichia coli* K12, Inheriting rfb-p3,4 Gene of *Shigella flexneri* as Revealed by Atomic Force Microscopy. *J. Microbiol. Epidemiol. Immunol. (Moscow)* **1997**, *6*, 15–18.
- (29) Boyle-Vavra, S.; Hahm, J.; Sibener, S. J.; Daum, R. S. Structural and Topological Differences between a Glycopeptide-Intermediate Clinical Strain and Glycopeptide-susceptible Strains of *Staphylococcus aureus* Revealed by Atomic Force Microscopy. *Antimicrob. Agents Chemother.* **2000**, *44*, 3456–3460.
- (30) Braga, P. C.; Ricci, D. Atomic Force Microscopy: Application to Investigation of *Escherichia coli* Morphology before and after Exposure to Cefodizime. *Antimicrob. Agents Chemother.* **1998**, *42*, 18–22.
- (31) Bolshakova, A. V.; Vorobyova, E. A.; Filonov, A. S.; Yaminsky I. V. Probe Microscopy of Soil Bacteria *Arthrobacter globiformis*. *Surf. Invest.* **2001**, *16*, 1789–1793.
- (32) Arnoldi, M.; Kacher, C.; Bäuerlein, E.; Radmacher, M.; Fritz, M. Elastic Properties of the Cell Wall of *Magnetospirillum Gryphiswaldense* Investigated by Atomic Force Microscopy. *Appl. Phys. A* **1997**, *66*, S613–S618.
- (33) Arnoldi, M.; Fritz, M.; Bauerlin E.; Radmacher, M.; Sackmann E.; Boulbitch, A. Bacterial Turgor Pressure Can Be Measured by Atomic Force Microscopy. *Phys. Rev. E* **2000**, *62*, 1034–1044.
- (34) Ong, Y.-L.; Razatos, A.; Georgiou, G.; Sharma, M. M. Adhesion Forces Between *E. coli* Bacteria and Biomaterial Surfaces. *Langmuir* **1999**, *15*, 2719–2725.
- (35) Lower, S. K.; Tadanier, C. J.; Hochella, M. F., Jr. Measuring Interfacial and Adhesion Forces Between Bacteria and Mineral Surfaces with Biological Force Microscopy. *Geochim. Cosmochim. Acta* **2000**, *64*, 3133–3139.
- (36) Auerbach, I. D.; Sorensen, C.; Hansma, H. G.; Holden, P. A. Physical Morphology and Surface Properties of Unsaturated *Pseudomonas putida* Biofilms. *J. Bacteriol.* **2000**, *182*, 3809–3815.
- (37) Boulbitch, A. Deformation of the Envelope of a Spherical Gram-negative Bacterium During the Atomic Force Microscopic Measurements. *J. Electron Microsc.* **2000**, *49*, 459–462.
- (38) Velegol, S. B.; Logan, B. E. Contributions of Bacterial Surface Polymers, Electrostatics, and Cell Elasticity to the Shape of AFM Force Curves. *Langmuir* **2002**, *18*, 5256–5262.
- (39) Landau, L. D.; Lifshitz, E. M. *Theory of Elasticity (Theoretical Physics, Vol. 7)*, 3rd ed.; Butterworth-Heinemann: Woburn, 1986.
- (40) Gallyamov, M. O.; Yaminsky, I. V. Quantitative Methods of Restoration of True Topographical Properties of the Objects by Measurement of AFM-images. 1. Contact Deformations of the Probe and the Specimen. *Surf. Invest.* **2001**, *16*, 1127–1134.
- (41) Thwaites, J. J.; Surana, U. C. Mechanical Properties of *Bacillus subtilis* Cell Walls: Effects of Removing Residual Culture Medium. *J. Bacteriol.* **1991**, *173*, 197–203.
- (42) Touhami, A.; Nysten, B.; Dufrene, Y. F. Nanoscale Mapping of the Elasticity of Microbial Cells by Atomic Force Microscopy. *Langmuir* **2003**, *19*, 4539–4543.
- (43) Xu, W.; Mulhern, P. J.; Blackford, B. L.; Jericho, M. H.; Firtel, M.; Beveridge, T. J. Modeling and Measuring the Elastic Properties of an Archaeal Surface, the Sheath of *Methanospirillum hugatei*, and the Implication for Methane Production. *J. Bacteriol.* **1996**, *178*, 3106–3112.
- (44) Yao, X.; Jericho, M.; Pink, D.; Beveridge, T. Thickness and Elasticity of Gram-Negative Murein Sacculi Measured by Atomic Force Microscopy. *J. Bacteriol.* **1999**, *181*, 6865–6875.
- (45) Chada, V. G. R.; Sanstad, E. A.; Wang, R.; Driks, A. Morphogenesis of Bacillus Spore Surfaces. *J. Bacteriol.* **2003**, *185*, 6255–6261.
- (46) Stemmer, A.; Engel, A. Imaging Biological Macromolecules by STM: Quantitative Interpretation of Topographs. *Ultramicroscopy* **1990**, *34*, 129–140.
- (47) Gallyamov, M. O.; Yaminskii, I. V. Quantitative Methods for Restoration of True Topographical Properties of Objects Using the Measured AFM-images. 2. The Effect of Broadening of the AFM-profile. *Surf. Invest.* **2001**, *16*, 1135–1141.
- (48) Velegol, S. B.; Pardi, S.; Li, X.; Velegol, D.; Logan, B. E. AFM Imaging Artifacts due to Bacterial Cell Height and AFM Tip Geometry. *Langmuir* **2003**, *19*, 851–857.
- (49) Bruinsma, G. M.; van der Mei, H. C.; Busscher, H. J. Bacterial Adhesion to Surface Hydrophilic and Hydrophobic Contact Lenses. *Biomaterials* **2001**, *22*, 3217–3224.
- (50) Filonov, A. S.; Gavrilko, D. Yu.; Yaminsky, I. V. *Scanning Probe Microscope Control and Image Processing Software "FemtoScan 001" Users Manual*; Advanced Technologies Center: Moscow, 2001 (<http://www.nanoscopy.net>).

Accepted for publication September 2, 2004.

BP049742C